J. Membrane Biol. 115, 71–81 (1990)

The Journal of
Membrane Biology

Aerolysin, a Hemolysin from *Aeromonas hydrophila*, Forms Voltage-Gated Channels in Planar Lipid Bilayers

H.U. Wilmsen†, F. Pattus†, and J.T. Buckley‡
†European Molecular Biology Laboratory, 6900 Heidelberg, Federal Republic of Germany, and ‡Department of Biochemistry and Microbiology, University of Victoria, Victoria, British Columbia, V8W 2Y2, Canada

Summary. The cytolytic toxin aerolysin was found to form ion channels which displayed slight anion selectivity in planar lipid bilayers. In voltage-clamp experiments the ion current flowing through the channels was homogeneous indicating a defined conformation and a uniform size. The channels remained open between −70 to +70 mV, but outside this range they underwent voltage-dependent inactivation which was observed as open-closed fluctuations at the single-channel level. Zinc ions not only prevented the formation of channels by inhibiting oligomerization of monomeric aerolysin but they also induced a closure of preformed channels in a voltage-dependent fashion. The results of a Hill plot indicated that 2–3 zinc ions bound to a site within the channel lumen. Proaerolysin, and a mutant of aerolysin in which histidine 132 was replaced by an asparagine, were both unable to oligomerize and neither could form channels. This is evidence that oligomerization is a necessary step in channel formation.

Key Words *Aeromonas hydrophila* · aerolysin · ionic channel · zinc ions · voltage dependence · planar lipid membranes

Introduction

Aeromonas hydrophila is a gram-negative bacterium which inhabits fresh water environments and is able to cause severe deep wound infections in humans [13, 16, 19, 26]. The organism releases a cytolytic protein of 50 kDa called aerolysin which appears to be largely responsible for its virulence. In recent years the mechanism of channel formation in cell membranes by aerolysin has been studied in some detail and the gene for the toxin has been cloned and sequenced [10, 24, 25]. The protein is very hydrophilic. Except within the signal sequence, it contains no hydrophobic sequences long enough to span a membrane in alpha helical form. No extensive regions of homology with other proteins have been observed.

There are two precursor forms of aerolysin. The first, preproaerolysin, contains the typical signal sequence of 23 amino acids [24] which is removed cotranslationally as the protein crosses the inner bacterial membrane [23, 24]. The resulting protoxin (proaerolysin) is the form exported from the bacteria. It is activated outside the cell by proteolytic removal of about 25 amino acids from the C-terminus [22] yielding the mature aerolysin. Aerolysin has been shown to bind to glycophorin on mammalian erythrocytes [21]. It then aggregates and forms 3-nm holes which destroy the membrane permeability barrier resulting in osmotic lysis [18]. Proaerolysin can also bind to erythrocyte membranes, but unlike aerolysin, it does not aggregate and, as this is an essential step in hole formation, it is unable to cause cytolysis [18]. The sequence of events of membrane penetration by the active toxin is not known, although there is some reason to believe that aerolysin oligomerizes before it completely inserts in the lipid bilayer [18]. It could be shown that histidine residues are necessary for the oligomerization process [18].

Studies of the properties of hole-forming toxins are often complicated by spontaneous and irreversible aggregation of the proteins at the concentrations needed to measure their interactions with model lipid membranes. A great advantage of the aerolysin system is the stability of the protoxin, which can be purified and activated under controlled conditions [7]. In this communication, we exploit this advantage and examine the channel-forming properties of aerolysin in model lipid membranes.

Materials and Methods

Purification of Aerolysin

Aerolysin and proaerolysin were purified from culture supernatants of *Aeromonas salmonicida* containing the cloned aerolysin

gene [39] essentially as described earlier [7]. Proaerolysin in which histidine 132 (His 132) was replaced by asparagine (Asn) by site-directed mutagenesis was purified the same way. Characterization of this mutant protein and details of its production will be presented elsewhere. Stock solutions of each of the proteins were stored at −60°C before use.

Planar Lipid Bilayer Experiments

Unless otherwise stated, the buffer used throughout was 1 M NaCl, 10 mM HEPES, 5 mM $CaCl_2$, pH 7.0–7.4. All solutions were prepared in double quartz-distilled water using reagent grade materials.

Phosphatidylcholine from soybeans (Sigma Chemical, St. Louis, MO, type IIS) was purified according to Kagawa and Racker [27]. Bilayers were formed across a 150-μm hole from 1-mg/ml solutions of the phospholipid as described by Schindler and Feher [35]. The hole was pretreated with a 1:40 solution of hexadecane in pentane before use.

The membrane voltage was clamped to the desired value using two Ag/AgCl electrodes connected to the buffer in the two compartments via agar bridges. The membrane current was amplified using an *I-V* converter with an operational amplifier (Burr Brown 3528) and feedback resistors ranging from 10^7 to 10^9 Ω. We term the sides of the membrane as the *cis* and *trans* compartments. The *trans* compartment was connected to the *I-V* converter and held at virtual ground potential. The sign of the membrane potential refers to the *cis* side of the membrane. Current was defined as positive when cations flowed into the *trans* compartment. Protein was always added to the *cis* side while the aqueous solution was stirred vigorously with a magnetic bar.

For ion selectivity measurements the *cis* compartment was perfused with a buffer containing 100 mM NaCl, 5 mM $CaCl_2$, 10 mM HEPES, pH 7.4 after channels had incorporated. Thus a 10-fold concentration gradient of NaCl was established which corresponded to about an 8.4- fold gradient in ion activity. The reversal potential was determined by applying a slow triangular wave voltage (2×10^{-3} Hz) using a function generator (Wavetek, model 143).

Results

Formation of Ion Channels

The results in Fig. 1*a* show the effect of aerolysin added to the *cis* side of a preformed planar lipid bilayer. After a lag of several minutes, membrane current increased rapidly in discrete steps, each representing the formation of a single ionic channel. The steps were quite homogeneous in size, implying that each channel carried the same amount of current. Hole formation did not affect bilayer stability, as membranes could be maintained for several hours.

In contrast to aerolysin, proaerolysin was unable to increase membrane current, even after long periods of exposure (Fig. 1*b*). However, adding trypsin to convert the protoxin to aerolysin resulted in a stepwise rise in current (after a lag of several minutes), similar to the increase observed with aerolysin in Fig. 1*a*. Trypsin itself was without effect on lipid bilayers. Similarly, no channel formation was ever observed with a mutant proaerolysin, in which His 132 was exchanged against Asn. This mutant was inactive, whether or not trypsin was present (*not shown*).

The single-channel current of aerolysin channels obtained from the incorporation curves such as those in Fig. 1*b* varied linearly with membrane voltage. The data points could be fitted to a straight line with a correlation coefficient of 0.99 in the voltage range from +120 to −120 mV, yielding a single-channel conductance $\lambda = 145$ and 420 pS in 300 mM and 1 M NaCl, respectively.

The results in Fig. 1*c* depict the incorporation of aerolysin over a longer period than was studied above. Following a lag after addition of protoxin and trypsin, the membrane current started to increase sharply. The rate of increase reached a maximum, $(dI/dt)_{max}$, and then declined. It was never reduced to zero, however, unless the hemolysin was removed from the aqueous solution by perfusion.

Voltage-Dependent Channel Inactivation

In order to study bilayers containing a fixed number of aerolysin channels, the bath solution on the *cis* side was exchanged with an aerolysin- and trypsin-free electrolyte solution after 300–1000 channels had incorporated. After this perfusion, there was no further increase in membrane current, confirming that aerolysin was the cause of channel formation. The response of these bilayers to membrane voltage steps up to ±50 mV is shown in Fig. 2*a*. Each time the voltage was changed, the membrane current immediately adopted a new value, which remained constant with time. The fact that a decline in current was never observed indicates that channel formation was irreversible. At higher voltages, slow, time-dependent channel inactivation did occur (Fig. 2*b*). Thus when the voltage was switched from 0 to +150 mV the membrane current immediately reached an initial peak value I_0 and then declined slowly, reaching a constant value I_∞. When the sign of the voltage was changed by switching from +150 to −150 mV, the same inactivation process could be observed. Finally, when the voltage was switched back to +150 mV again, the original peak value of the first voltage jump was reached. The reversibility of voltage inactivation suggests that current inactivation was caused by changes in the ability of channels to conduct ions and not by a loss of channels from the bilayer.

The membrane current almost immediately returned to the initial peak value I_0 of the fully activated channels, when the voltage sign was changed

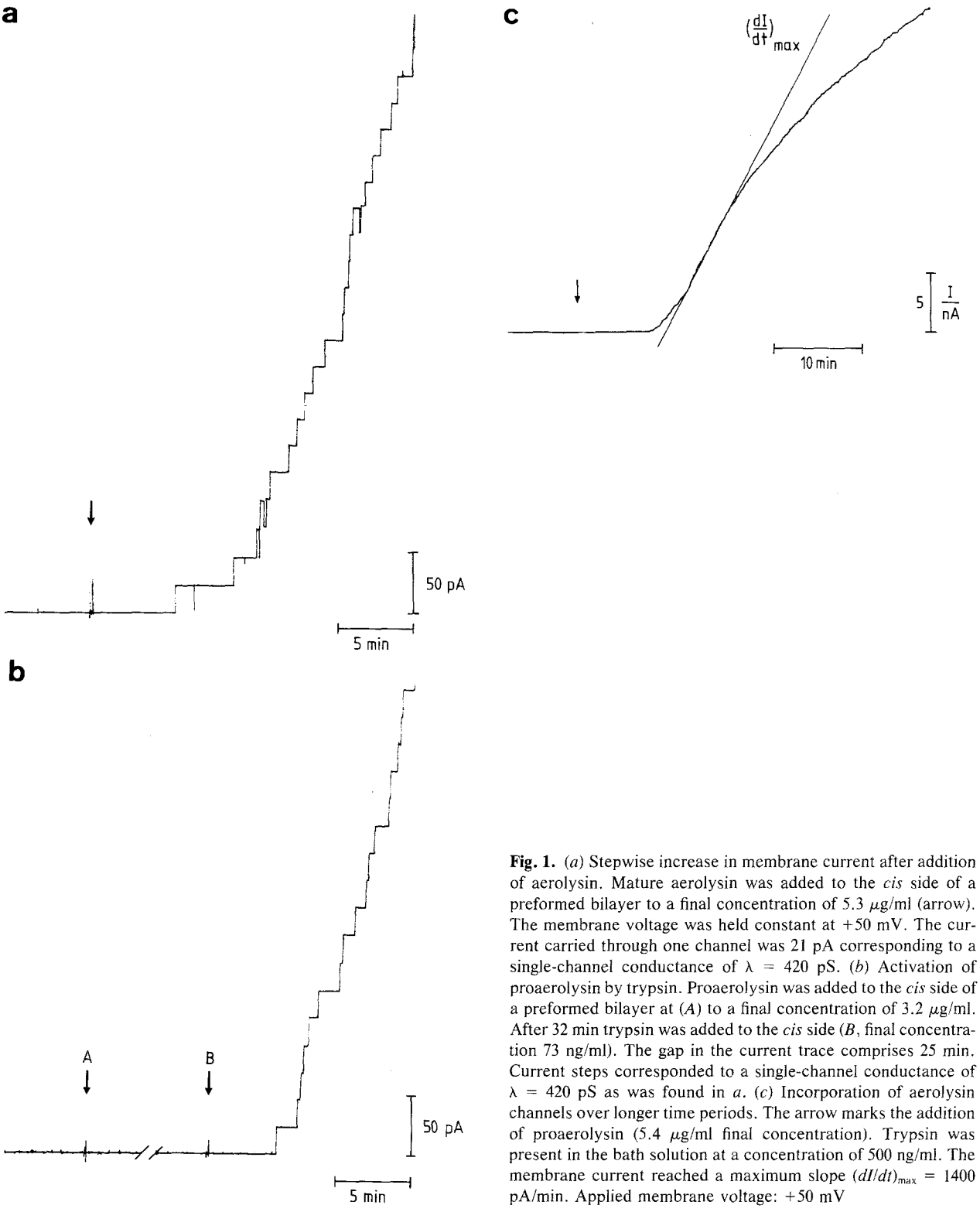

Fig. 1. (*a*) Stepwise increase in membrane current after addition of aerolysin. Mature aerolysin was added to the *cis* side of a preformed bilayer to a final concentration of 5.3 μg/ml (arrow). The membrane voltage was held constant at +50 mV. The current carried through one channel was 21 pA corresponding to a single-channel conductance of λ = 420 pS. (*b*) Activation of proaerolysin by trypsin. Proaerolysin was added to the *cis* side of a preformed bilayer at (*A*) to a final concentration of 3.2 μg/ml. After 32 min trypsin was added to the *cis* side (*B*, final concentration 73 ng/ml). The gap in the current trace comprises 25 min. Current steps corresponded to a single-channel conductance of λ = 420 pS as was found in *a*. (*c*) Incorporation of aerolysin channels over longer time periods. The arrow marks the addition of proaerolysin (5.4 μg/ml final concentration). Trypsin was present in the bath solution at a concentration of 500 ng/ml. The membrane current reached a maximum slope $(dI/dt)_{max}$ = 1400 pA/min. Applied membrane voltage: +50 mV

(*see* Fig. 2*b*). This must mean that the inactivated channels were completely reactivated before they were inactivated anew. Under the conditions described in Fig. 2*b* reactivation took place in a few milliseconds or less, much less time than was required for inactivation.

A semilogarithmic plot of the time course of current inactivation in Fig. 2*b* revealed that it did

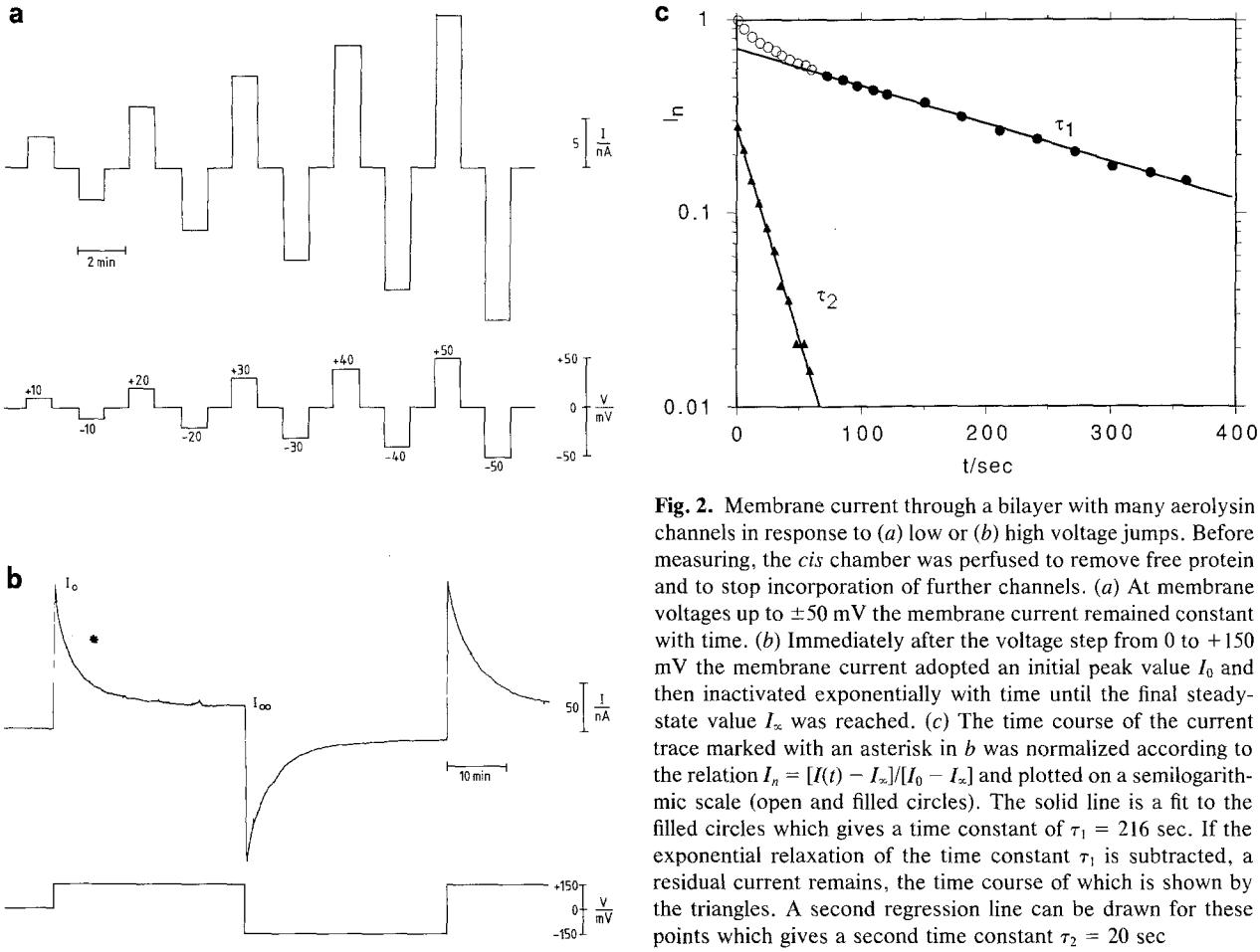

Fig. 2. Membrane current through a bilayer with many aerolysin channels in response to (*a*) low or (*b*) high voltage jumps. Before measuring, the *cis* chamber was perfused to remove free protein and to stop incorporation of further channels. (*a*) At membrane voltages up to ±50 mV the membrane current remained constant with time. (*b*) Immediately after the voltage step from 0 to +150 mV the membrane current adopted an initial peak value I_0 and then inactivated exponentially with time until the final steady-state value I_∞ was reached. (*c*) The time course of the current trace marked with an asterisk in *b* was normalized according to the relation $I_n = [I(t) - I_\infty]/[I_0 - I_\infty]$ and plotted on a semilogarithmic scale (open and filled circles). The solid line is a fit to the filled circles which gives a time constant of $\tau_1 = 216$ sec. If the exponential relaxation of the time constant τ_1 is subtracted, a residual current remains, the time course of which is shown by the triangles. A second regression line can be drawn for these points which gives a second time constant $\tau_2 = 20$ sec

not follow a single exponential function, but could be fitted well by two exponential components with two time constants τ_1 and τ_2 (Fig. 2*c*).

Figure 3 shows inactivation and reactivation at the single-channel level. A voltage step from +50 to +175 mV induced stepwise closing of channels and a subsequent voltage switch to −50 mV clearly promoted reopening. In contrast to the reactivation shown in Fig. 2*b*, the time course of the reactivation process at −50 mV was well resolved. This indicates that the velocity of reactivation is voltage-dependent and slower at −50 than at −150 mV. The closing of single channels was independent of the polarity of the applied voltage, as similar stepwise decreases of the membrane current could also be observed at negative voltages <−70 mV (*not shown*). Thus aerolysin channels switch between conducting (open) and nonconducting (closed) states in a voltage-dependent fashion regardless of polarity.

The ratio between the steady-state value I_∞ and the initial peak value I_0 in Fig. 2*b* is the fraction of channels which were not inactivated at a given voltage. Figure 4 shows this ratio plotted against the applied membrane voltage. A bell-shaped curve was obtained which was fairly symmetrical with respect to the *y*-axis. In the range −70 to +70 mV, I_∞/I_0 was 1, i.e., no inactivation of the membrane current occurred. However, small voltage changes outside this range resulted in sharp decreases in I_∞/I_0. The switching voltages V_0, at which 50% of the ion channels were inactivated, were +94 and −94 mV, respectively.

The activation/inactivation process was not dependent on the presence of Ca^{2+} ions in the salt solution. In the absence of Ca^{2+} ions, the I_∞/I_0 curve retained its symmetrical bell-shaped form without any significant changes in the V_0 values (Fig. 4). Similarly, Mg^{2+} ions did not affect the voltage-dependent inactivation (*not shown*).

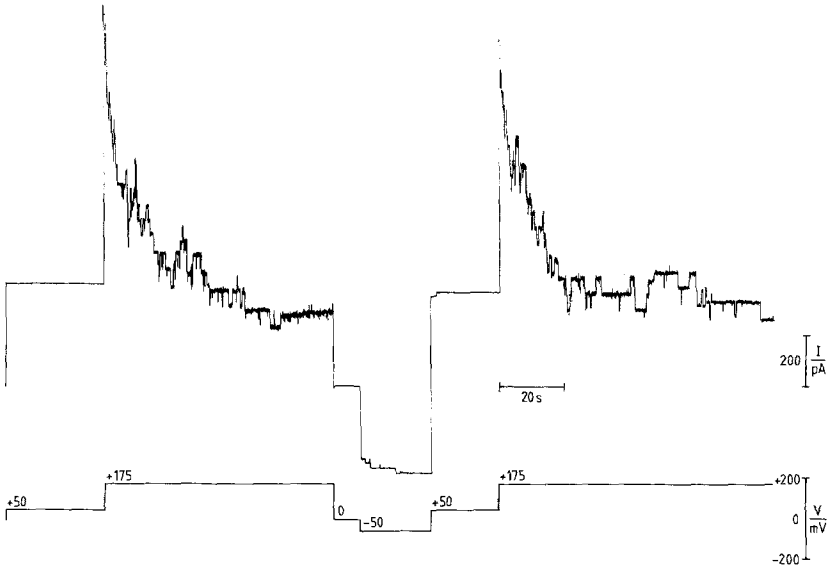

Fig. 3. Closing of single aerolysin channels at high membrane potentials. Only few channels were allowed to incorporate into a bilayer before perfusion. Note by comparing with Fig. 2*b* that the time course of this reactivation was much slower than at −150 mV and that the kinetics of inactivation at +175 mV are much faster than at 150 mV. This implies that the kinetics of inactivation and reactivation of aerolysin channels are voltage dependent

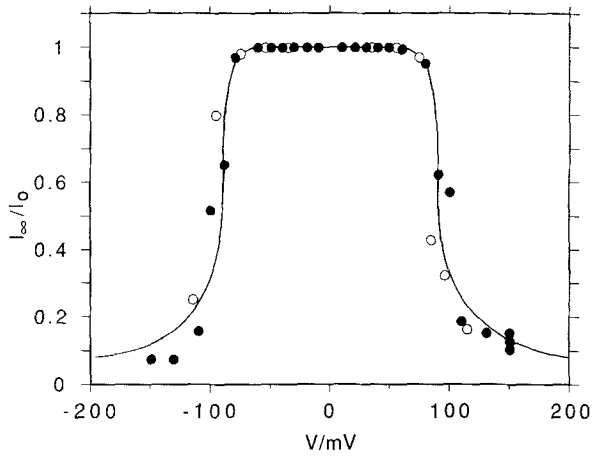

Fig. 4. I_∞/I_0 as a function of the final membrane voltage. I_∞ and I_0 were determined in voltage jump experiments as shown in Fig. 2*b*. The membrane voltage was switched from a value at which all channels were activated to the final voltage value. The V_0 values at which 50% inactivation was reached were +94 and −94 mV, respectively. The filled symbols represent experiments in the presence of 5 mM $CaCl_2$. The open symbols show experiments in which the salt solution contained 1 mM EDTA instead of $CaCl_2$

The Effect of Zinc Ions

Bashford et al. [3] have shown that the permeabilizing effects of a series of cytolysins and cytotoxic agents on cells can be inhibited by divalent cations with Zn^{2+} being the most effective. We therefore investigated whether Zn^{2+}, in contrast to Mg^{2+} or Ca^{2+}, had any effect on the formation of aerolysin channels or on preformed channels. The results in Fig. 5*a* show that when Zn^{2+} was present in the buffer it prevented the increase in bilayer current which normally followed addition of proaerolysin and trypsin. However, removal of the divalent cation, free aerolysin and trypsin by perfusion resulted in an *S*-shaped increase in membrane current similar to that observed in Fig. 1*c*, except that the current reached a constant value after about 14 min.

The effect of adding Zn^{2+} to the *cis* side of a bilayer containing preformed aerolysin channels is shown in Fig. 5*b*. The channels were first incorporated in the absence of Zn^{2+}, and the *cis* compartment was perfused to remove free aerolysin before the divalent cation was added. Zn^{2+} caused the current to decrease rapidly at an applied voltage of +50 mV until it reached a constant value which was about 3% of the membrane current before addition. Perfusing the chamber to remove Zn^{2+} resulted in an immediate one-step return of the current to its original value when the voltage was switched back to +50 mV. Similar results were obtained when Zn^{2+} was added on the *trans* side of the bilayer at a membrane voltage of −50 mV (*not shown*). Figure 6*a* shows the effect of Zn^{2+} when a membrane contained only a few preformed aerolysin channels. It may be seen that the drop of membrane current after addition of Zn^{2+} was due to an all-or-none closure of the channels and not to a reduction of the single-channel conductance of the open state.

The results in Fig. 6*b* show the changes in current which occurred in response to voltage changes to −50 and +50 mV, respectively, in the presence of 1 mM Zn^{2+} on the *cis* side of a membrane containing aerolysin channels. When the voltage was

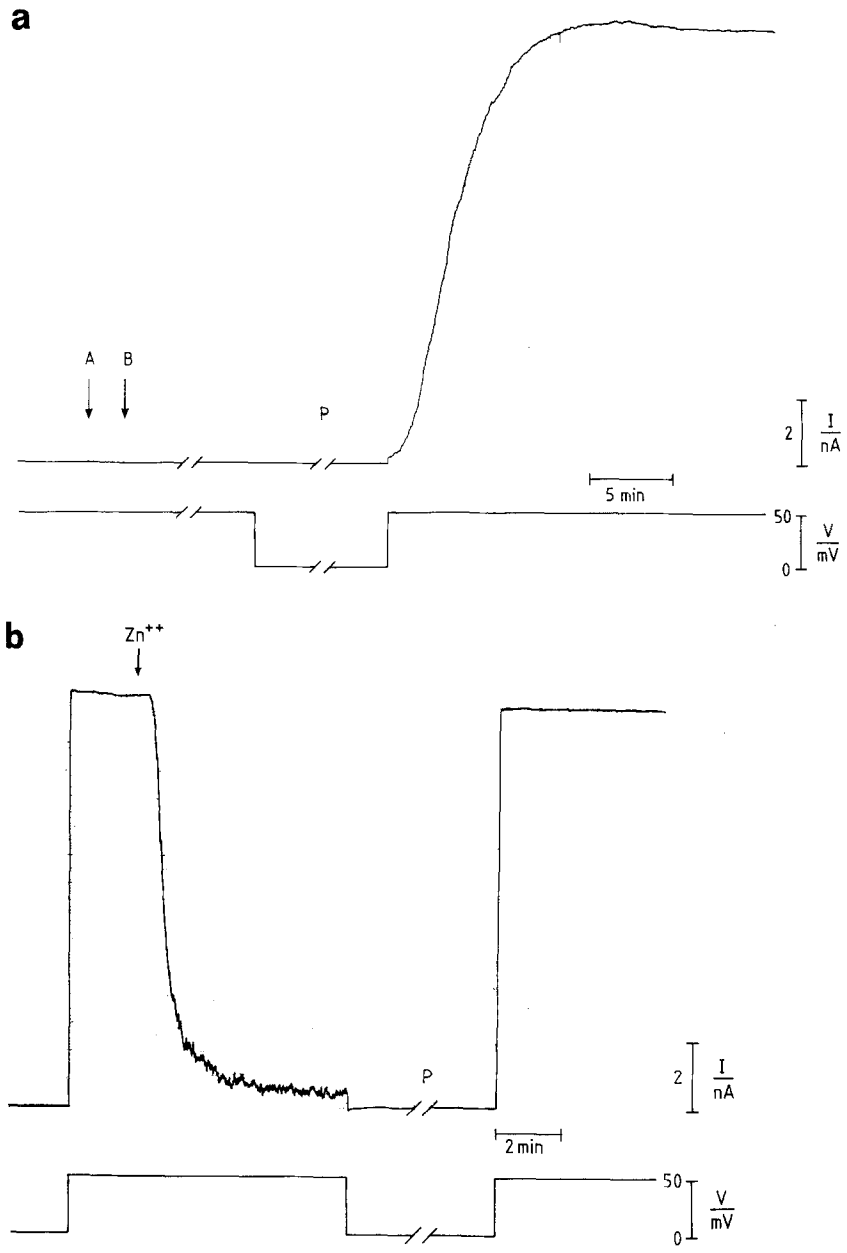

Fig. 5. (*a*) Zn^{2+} in the aqueous solution prevents the formation of aerolysin channels. At the beginning of the trace Zn^{2+} was added to the *cis* side to a final concentration of ≈3 mM (arrow *A*). This was followed by the simultaneous addition of proaerolysin and trypsin (5.8 μg/ml and 200 ng/ml, respectively; arrow *B*). Membrane voltage was kept at +50 mV for 67 min. At (*P*) the *cis* side was perfused to remove Zn^{2+} ions, trypsin, free proaerolysin and aerolysin. Note that the membrane current increased slowly in an *S*-shaped curve. (*b*) The effect of Zn^{2+} ions on preformed aerolysin channels. The *cis* chamber was perfused before this experiment to stop incorporation of further channels. The trace starts with a current step through a membrane containing many aerolysin channels when the voltage is switched from 0 to +50 mV. When Zn^{2+} was added to the *cis* side (arrow; final concentration 3.7 mM) the membrane current decreased drastically and reached a final steady-state value. After perfusion (*P*) to remove Zn^{2+} again, the current instantly reached the original value without any delay when the voltage was switched on again

switched to −50 mV, the membrane current immediately attained a constant value. However, when the voltage was switched to +50 mV, the current decreased exponentially after reaching its initial value. It appears therefore that the voltage range in which inactivation of the membrane current occurs is lower on the positive side of the voltage axis in the presence of Zn^{2+} in the *cis* compartment. Thus the relation I_∞/I_0 is no longer symmetrical. This is clarified in Fig. 7, where I_∞/I_0 is shown as a function of voltage at three different concentrations of Zn^{2+}. Higher Zn^{2+} concentrations lowered the voltage range at which current inactivation occurred on the positive side of the voltage axis. On the negative side, however, the voltage-dependent inactivation of the membrane current remained unaltered. This change on the positive side of the voltage axis can be described by the shift of the switching voltage V_0 to lower membrane voltages as the concentration of Zn^{2+} is increased on the *cis* side of the bilayer (Fig. 7).

The inactivating effect of Zn^{2+} on aerolysin channels is concentration dependent. In Fig. 8*a*, the relation I_∞/I_0 at a constant membrane voltage of +50

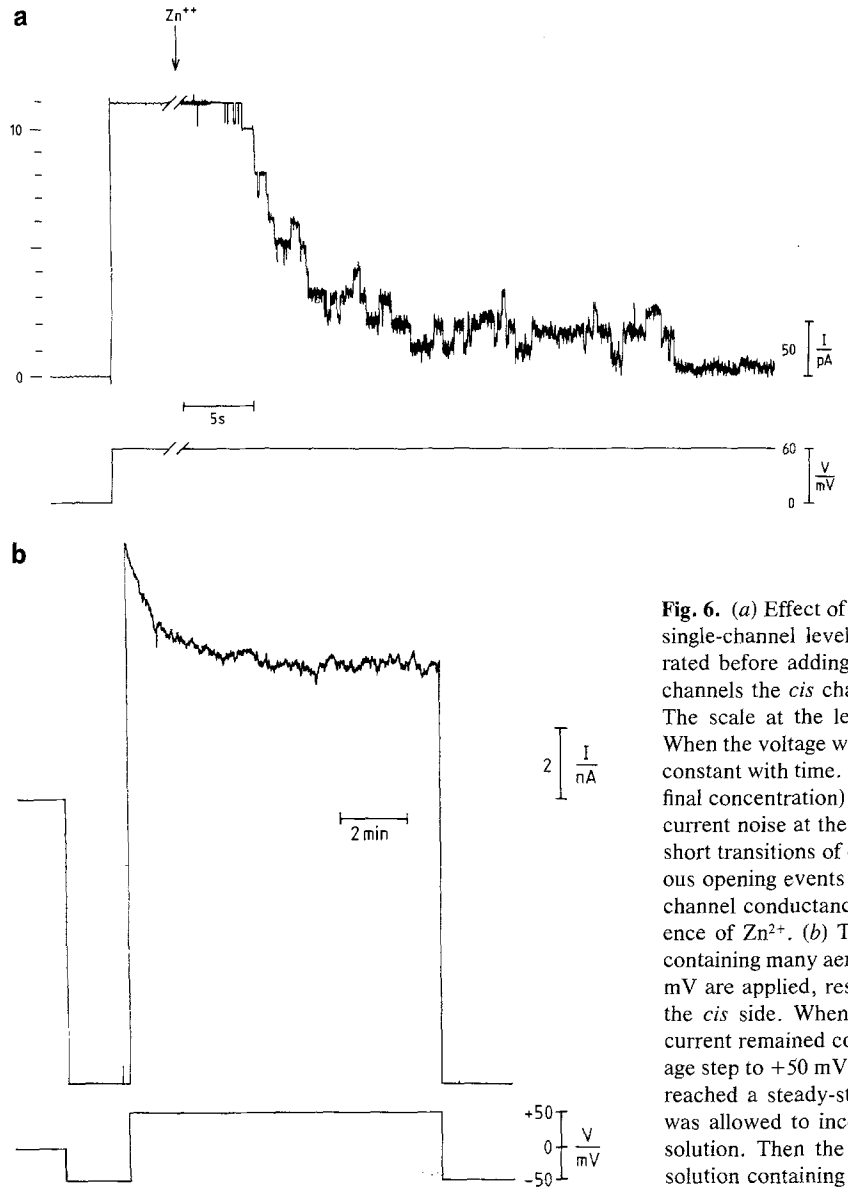

Fig. 6. (*a*) Effect of Zn^{2+} on preformed aerolysin channels at the single-channel level. Eleven aerolysin channels were incorporated before adding Zn^{2+}. To stop the incorporation of further channels the *cis* chamber was perfused before this experiment. The scale at the left marks the single-channel current levels. When the voltage was switched to +60 mV the current remained constant with time. After addition of Zn^{2+} to the *cis* side (≈3 mM final concentration) the channels started to close. The increased current noise at the end of the trace may have been due to very short transitions of closed channels to the open state. Spontaneous opening events at the end of the trace show that the single-channel conductance was not changed significantly in the presence of Zn^{2+}. (*b*) The membrane current through a membrane containing many aerolysin channels is shown when +50 and −50 mV are applied, respectively, in the presence of 1 mM Zn^{2+} on the *cis* side. When the voltage was switched to −50 mV the current remained constant and did not alter with time. The voltage step to +50 mV resulted in a slow inactivating current which reached a steady-state value. Before the experiment aerolysin was allowed to incorporate into the bilayer in a Zn^{2+}-free salt solution. Then the *cis* compartment was perfused with a salt solution containing 1 mM Zn^{2+}

mV is plotted against the Zn^{2+} concentration. A sigmoidal dose-response curve is obtained. The apparent dissociation constant is about 0.9 mM at this voltage.

Figure 8*a* can be rearranged in a Hill plot if we assume that the relation N_c/N_o between the number N_c of channels that were closed by Zn^{2+} and the number of channels which remained open, N_o, is represented by the relation $[I_0 - I_\infty]/I_\infty$. In Fig. 8*b*, in which N_c/N_o is plotted against the Zn^{2+} concentration on a double-logarithmic scale, the data points can be fitted fairly well be a straight line; the slope of which (Hill coefficient) is 2.5. This implies that at least 2–3 ions have to bind to the channel to close it.

Ion Selectivity

The ion selectivity of aerolysin channels was determined using a 10-fold concentration gradient of NaCl across the membrane (*see* Materials and Methods). Depending on the permeability ratio b between Na^+ and Cl^-, a reversal potential E_{rev} develops across the membrane the magnitude of which is given by the Goldman-Hodgkin-Katz equation:

$$E_{rev} = \frac{RT}{F} \ln \frac{b\alpha^c_{Na} + \alpha^i_{Cl}}{b\alpha^i_{Na} + \alpha^c_{Cl}}.$$

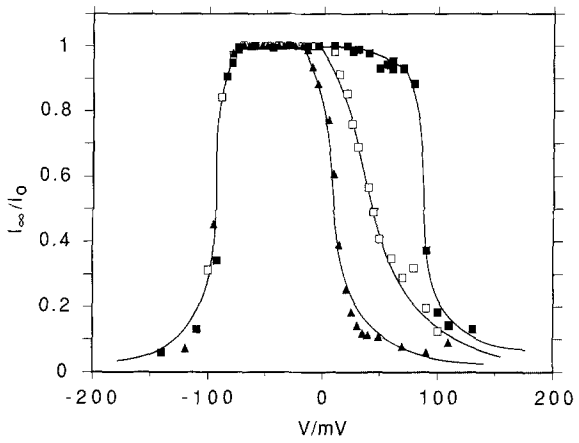

Fig. 7. I_∞/I_0 in aerolysin-containing membranes as a function of membrane voltage at three Zn^{2+} concentrations on the *cis* side. The symbols are: ■ = 0.25 mM Zn^{2+}; □ = 1.0 mM Zn^{2+}; ▲ = 2.0 mM Zn^{2+}. The V_0 values in the positive voltage range are in the order of increasing Zn^{2+} concentration: +86; +46; +12 mV. Note that the V_0 value in the negative voltage range is not affected by the presence of Zn^{2+} on the *cis* side

α^c and α^t are the ion activities on the *cis* and *trans* side, respectively. E_{rev} was determined as that voltage at which the net current became zero when a triangular wave voltage was applied. At pH 7.4 a reversal potential of −24 mV was obtained which corresponds to a Cl^-/Na^+-permeability ratio of about $b = 3.6:1$.

Discussion

Many of the observations concerning channel formation made here support the results of earlier studies with aerolysin using erythrocytes. Thus Howard and Buckley [21] concluded that aerolysin forms well-defined holes in the cell membrane of erythrocytes and we have found uniform channels in planar lipid bilayers. With the protein concentration used in these studies (3–6 μg/ml) we can estimate that channel densities of 3–4 × 10^6 per cm^2 were obtained 30 min after the onset of channel formation. Rat erythrocytes incubated with concentrations of aerolysin four orders of magnitude lower than we have used bind far more aerolysin. However, the differences in affinity and membrane concentration are almost certainly due to the presence on the cell surface of glycophorin which acts as a receptor for the toxin thereby increasing local concentration and the rate of aggregation and insertion. There is clearly no absolute requirement for glycophorin, as not only do we see channel formation in pure lipid bilayers, but also Howard and Buckley reported hole formation in phospholipid vesicles [21].

Proaerolysin, which Garland and Buckley have shown is inactive because it cannot aggregate [18], is unable to form channels in lipid bilayers unless it is converted to aerolysin with trypsin. In addition, aerolysin in which His 132 is replaced by an Asn also cannot form channels. This corresponds with earlier observations, showing that histidine residues are necessary for aggregation and cytolytic activity [18]. Taken together, these results, and those described below with Zn^{2+}, indicate that aerolysin oligomerization is an indispensable requirement for the formation of ion-permeable channels in planar lipid bilayers as well as in cell membranes. Indeed, it seems very likely that the aerolysin oligomer is the channel itself. From our experiments we cannot deduce how many monomers are required to form a functional oligomer; however, aerolysin oligomers migrate with an apparent molecular mass of 275 kDa during SDS-PAGE (oligomers are stable to boiling in SDS-mercaptoethanol), suggesting they are pentameric or hexameric [18].

The lag period which preceded channel formation was approximately the same whether aerolysin, or proaerolysin together with trypsin were added. This shows that activation of the protoxin by trypsin was not limiting. In fact rough calculations indicate that the lag preceding channel formation is largely attributable to the diffusion time of the protein through the unstirred water layer next to the membrane [1, 8].

The current through a bilayer membrane containing many aerolysin channels underwent inactivation in response to voltage steps to values outside the range of ±70 mV. The relation between the steady-state current value and the initial peak value as a measure of the fraction of open channels depended on the applied membrane voltage and followed a symmetrical bell-shaped curve. Single-channel experiments showed that the inactivation of the macroscopic membrane current was caused by a voltage-dependent closing reaction of the channels.

In this study we could demonstrate two separate effects of Zn^{2+} on aerolysin, one on channel assembly and another on preformed channels. Concentrations of Zn^{2+} as low as 3 mM were sufficient to inhibit channel formation completely. However, when the bath medium was exchanged to remove Zn^{2+} and free protein, the membrane current increased in an *S*-shaped fashion with time. This implies that proaerolysin was normally processed by trypsin during the incubation with Zn^{2+} and that aerolysin had attached to the lipid bilayer where it remained after the perfusion. Activation of proaero-

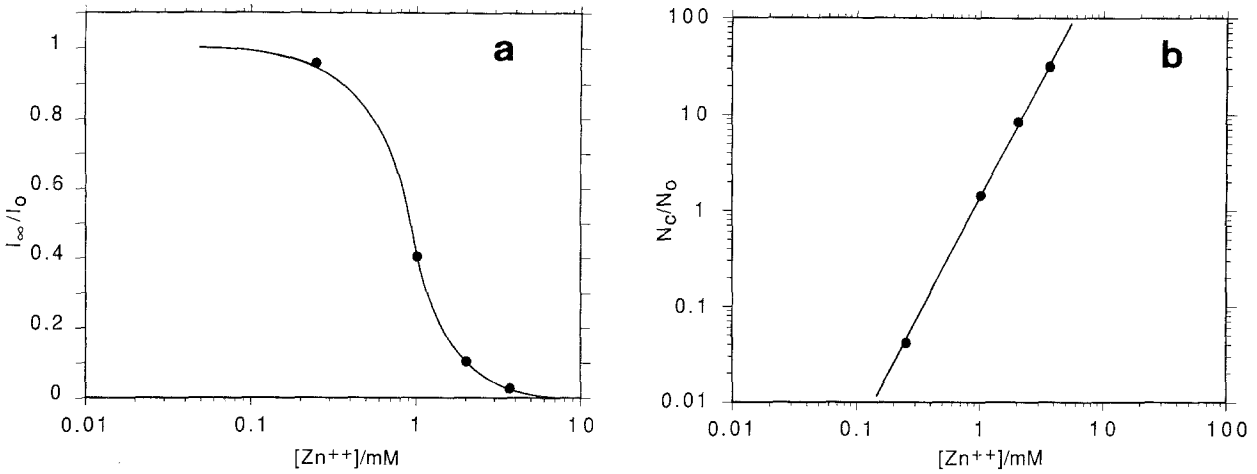

Fig. 8. (*a*) The relation I_∞/I_0 at a constant membrane voltage of +50 mV is plotted against the Zn^{2+} concentration. The data points were taken from Fig. 7. A sigmoidal dose-response curve is obtained with an apparent dissociation constant K_d = 0.9 mM. (*b*) The relation N_c/N_0 between the numbers of closed and open channels at a constant membrane voltage of +50 mV is plotted *versus* the Zn^{2+} concentration on a double-logarithmic scale (Hill plot). The data points were taken from Fig. 8*a*. The straight line is a least-squares fit and has a slope of 2.5

lysin under these conditions was confirmed by SDS-PAGE (*not shown*). Although these results show that aerolysin can bind to the bilayer, they do not necessarily mean that the protein had completely inserted. The time-dependent *S*-shaped increase in the membrane current presumably represents events which occurred after activation and binding. One such event may be the oligomerization of bound aerolysin molecules. The onset of channel activity would then mark the insertion of the channel-forming oligomer into the membrane. This mechanism is consistent with the observations by Garland and Buckley [18], which indicated that aerolysin oligomerizes before it enters the lipid bilayer. Thus the *S*-shaped increase in membrane current reflects a genuine *de-novo* formation of channels. The tight binding of monomers to the bilayer-water interface must facilitate the oligomerization reaction at the membrane level because a high two-dimensional concentration of oriented monomers must arise. Zn^{2+} would inhibit channel formation by interacting with attached monomers and preventing oligomerization.

In addition to its effect on aggregation, Zn^{2+} also blocked preformed channels in the bilayer (Fig. 5*b*). The membrane current returned instantly to its original level when the ion was removed by perfusion. This effect is therefore different from that shown in Fig. 5*a*, where a slow, *S*-shaped current increase appears to represent *de-novo* formation of channels after removal of Zn^{2+}. Thus we can conclude that Zn^{2+} does not disassemble preformed conducting aerolysin aggregates and that no new channels are formed when it is removed.

The effect of Zn^{2+} on preformed channels depended on both the transmembrane voltage and the concentration of the divalent metal ion. This is shown in Fig. 7. In the presence of Zn^{2+} the switching voltage V_0 (at which 50% inactivation was reached), was shifted to less positive values in the positive voltage range. In contrast to this, the inactivation behavior at negative voltages remained unaffected and no shift of V_0 occurred in this voltage range. This may indicate that Zn^{2+} must move partway across the electric field in the lumen of preformed aerolysin channels to cause current inactivation. Only if the *cis* side is held at positive potentials can Zn^{2+} ions move into the channel lumen and close it. Conversely, when the *cis* side is held at a negative potential, the blocking metal ion is repelled back into the bulk solution by the electric field. The notion of such a voltage-dependent blockade mechanism is supported by the observation that aerolysin channels can also be blocked efficiently by Zn^{2+} ions from the *trans* side. However, in this case negative voltages (*trans* side positive) have to be applied. Obviously, Zn^{2+} ions interfere with specific sites on the protein. These sites must face the inside of the aqueous channel lumen in the ion-conducting oligomer and must be localized some distance from the channel mouth.

An alternative mechanism involving binding sites outside the channel lumen may also be envisaged. Such a blockade model was proposed for *Staphylococcus aureus* alpha toxin [29] in order to account for the blockade mechanism of polyvalent metal ions. However, this mechanism is fundamentally different from that observed with aerolysin

(*see* next section) and the model described above for aerolysin appears more plausible since it explains satisfactorily the voltage dependence of the Zn^{2+}-induced blockade as well as the blockade from both sides.

When only a few aerolysin channels were present it could be shown that the inactivating effect of Zn^{2+} ions was due to an all-or-none closure of the channels and not to a gradual decrease of the single-channel conductance as has been described in the case of other voltage-dependent blockade mechanisms [12]. Since the integrity of the channel-forming oligomer appears to be unaffected by Zn^{2+} ions it is likely that the channel closure is due to a steric rearrangement of the subunits. A model of this kind has been proposed for the gap junction channel which is made up of an annulus of six monomers delineating a narrow channel through the membrane [38].

Comparison of Aerolysin with Other Bacterial Toxins and Porins

The channel-forming properties of the cytolytic alpha toxin from *Staphylococcus aureus* and the hemolysin from *E. coli* have also been described in detail [29, 30] and aerolysin seems to share more properties with the former. Oligomerization of monomers is a prerequisite for the cytolytic activity of both aerolysin and alpha toxin [2, 5, 6, 15, 17, 37]. Moreover, the amino acid sequences of both proteins contain large amounts of hydrophilic amino acids and are devoid of long hydrophobic stretches [20]. CD-spectroscopy studies indicate that both toxins have high beta sheet content [37, J.T. Buckley, *unpublished observations*]. In contrast, the asymmetric voltage dependence and the type of amino acid sequence of *E. coli* hemolysin are most similar to those of colicins [11, 30, 34] and like colicins, *E. coli* hemolysin most probably belongs to the alpha-helical type of pore-forming proteins.

The channel-forming properties of aerolysin and alpha toxin differ in several respects in spite of the similarities above. Alpha-toxin channels are inactivated by membrane voltage only if divalent cations are present, whereas aerolysin channels display a pronounced voltage dependence with and without divalent cations (Fig. 4). The channels are also fundamentally different as the voltage dependence of alpha-toxin channels is inverse to that of aerolysin channels if blocking metal ions are present on one side of the bilayer only. As a result, a binding site for ions inside the alpha toxin channel lumen has been ruled out and it has been concluded that metal ions bind to at least two different and independent sites at both ends of the channel outside its lumen [29]. In contrast, our data suggest that the Zn^{2+} binding site is localized within the aerolysin channel lumen.

Our experience working with channel-forming proteins and the results of others lead to the conclusion that symmetrical inactivation by membrane potential and bell-shaped current-voltage curves are typical properties of ion-channels of the "porin type." These proteins, which are found in the outer membranes of gram-negative bacteria and mitochondria, contain large portions of beta sheet secondary structure and their amino acid sequences reveal high proportions of hydrophilic amino acids [14, 31–33, 36]. Porins form large water-filled channels in planar lipid bilayer membranes and, like aerolysin, characteristically show high single-channel conductances [4]. Although these common properties could be circumstantial they may indicate that channel formers of this class share a common design, as has been pointed out for eucaryotic alpha-helical voltage-dependent channels [9]. Because aerolysin shares all of these properties, it is conceivable that it is related to an *Aeromonas* porin as was postulated earlier [21]. The fact that there is presently no obvious homology to the porins that have been sequenced is not surprising, as their primary structures are not well-conserved between species, and in addition, the primary structure of none of the *Aeromonas* porins is known. Recently crystals of porins [28] as well as proaerolysin have been obtained which are suitable for X-ray crystallography (A. Tucker, *personal communication*). As a result the prospects are rather good that increased understanding of their molecular structures will determine if these channel formers have a common design.

This work was supported by postdoctoral fellowships from EMBL and the Deutsche Forschungsgemeinschaft (Wi 872/2-1). We would like to thank J.H. Lakey for helpful discussions.

References

1. Andreoli, T.E., Troutman, S.L. 1971. An analysis of unstirred layers in series with "tight" and "porous" lipid bilayer membranes. *J. Gen. Physiol.* **57**:464–478
2. Arbuthnott, J.P., Freer, J.H., Billcliffe, B. 1973. Lipid-induced polymerization of staphylococcal α-toxin. *J. Gen. Microbiol.* **75**:309–319
3. Bashford, C.L., Alder, G.M., Menestrina, G., Micklem, K.J., Murphy, J.J., Pasternak, C.A. 1986. Membrane damage by hemolytic viruses, toxins, complement, and other cytotoxic agents. *J. Biol. Chem.* **261**:9300–9308
4. Benz, R., Bauer, K. 1988. Permeation of hydrophilic mole-

cules through the outer membrane of gram-negative bacteria. *Eur. J. Biochem.* **176:**1–19
5. Bhakdi, S., Füssle, R., Tranum-Jensen, J. 1981. Staphylococcal α-toxin: Oligomerization of hydrophilic monomers to form amphiphilic hexamers induced through contact with deoxycholate detergent micelles. *Proc. Natl. Acad. Sci. USA* **78:**5475–5479
6. Bhakdi, S., Tranum-Jensen, J. 1987. Damage to mammalian cells by proteins that form transmembrane pores. *Rev. Physiol. Biochem. Pharmacol.* **107:**147–223
7. Buckley, J.T., Howard, S.P. 1988. Aerolysin from *Aeromonas hydrophila*. *Methods Enzymol.* **165:**193–199
8. Cass, A., Finkelstein, A. 1967. Water permeability of thin lipid membranes. *J. Gen. Physiol.* **50:**1765–1784
9. Catterall, W.A. 1988. Structure and function of voltage-sensitive ion channels. *Science* **242:**50–61
10. Chakraborty, T., Huhle, B., Bergbauer, H., Goebel, W. 1986. Cloning, expression, and mapping of the *Aeromonas hydrophila* aerolysin gene determinant in *Escherichia coli* K-12. *J. Bacteriol.* **167:**368–374
11. Collarini, M., Amblard, G., Lazdunski, C., Pattus, F. 1987. Gating processes of channels induced by colicin A, its C-terminal fragment and colicin E1 in planar lipid bilayers. *Eur. Biophys. J.* **14:**147–153
12. Coronado, R., Miller, C. 1979. Voltage-dependent caesium blockade of a cation channel from fragmented sarcoplasmatic reticulum. *Nature (London)* **280:**807–810
13. Daily, O.P., Joseph, S.W., Coolbaugh, J.C., Walker, R.I., Merrell, B.R., Rollins, D.M., Seidler, R.J., Colwell, R.R., Lissner, C.R. 1981. Association of *Aeromonas sobria* with human infection. *J. Clin. Microbiol.* **13:**769–777
14. Forte, M., Gay, H.R., Manella, C.A. 1987. Molecular genetics of the VDAC ion channel: Structural model and sequence analysis. *J. Bioenerg. Biomembr.* **19:**341–350
15. Freer, J.H., Arbuthnott, J.P., Bernheimer, A.W. 1968. Interaction of staphylocccal α-toxin with artificial and natural membranes. *J. Bacteriol.* **95:**1153–1168
16. Freij, B.J. 1984. *Aeromonas:* Biology of the organism and diseases of children. *Pediatr. Infect. Dis.* **3:**164–175
17. Füssle, R., Bhakdi, S., Sziegoleit, A., Tranum-Jensen, J., Kranz, T., Wellensiek, H.J. 1981. On the mechanism of membrane damage by *Staphylococcus aureus* α-toxin. *J. Cell Biol.* **91:**83–94
18. Garland, W.J., Buckley, J.T. 1988. The cytolytic toxin aerolysin must aggregate to disrupt erythrocytes, and aggregation is stimulated by human glycophorin. *Infect. Immunol.* **56:**1249–1253
19. Gracey, M., Burke, V., Robinsin, J. 1982. *Aeromonas* associated gastroenteritis. *Lancet* **ii:**1304–1306
20. Grant, G.S., Kehoe, M. 1984. Primary sequence of the alpha toxin gene from *Staphylococcus aureus* Wood 46. *Infect. Immunol.* **46:**615–618
21. Howard, S.P., Buckley, J.T. 1982. Membrane glycoprotein receptor and hole-forming properties of a cytolytic protein. *Biochemistry* **21:**1662–1667
22. Howard, S.P., Buckely, J.T. 1985*a*. Activation of the hole-forming toxin aerolysin by extracellular processing. *J. Bacteriol.* **163:**336–340
23. Howard, S.P., Buckley, J.T. 1985*b*. Protein export by a gram-negative bacterium. Production of aerolysin by *Aeromonas hydrophilia*. *J. Bacteriol.* **161:**1118–1124
24. Howard, S.P., Buckley, J.T. 1986. Molecular cloning and expression in *Escherichia coli* of the structural gene for the hemolytic toxin aerolysin from *Aeromonas hydrophila*. *Mol. Gen. Genet.* **204:**289–295
25. Howard, S.P., Garland, W.J., Green, M.J., Buckley, J.T. 1987. Nucleotide sequence of the gene for the hole-forming toxin aerolysin of *Aeromonas hydrophila*. *J. Bacteriol.* **169:**2869–2871
26. Janda, J.M., Bottone, E.J., Sinner, C.V., Calcaterra, D. 1983. Phenotypic markers associated with gastrointestinal *Aeromonas hydrophilia* isolates from symptomatic children. *J. Clin. Microbiol.* **17:**588–591
27. Kagawa, Y., Racker, E. 1971. Partial resolution of the enzymes catalyzing oxidative phosphorylation: XXV. Reconstitution of particles catalyzing $^{32}P_i$-adenosine triphosphate exchange. *J. Biol. Chem.* **246:**5477–5487
28. Kleffel, B., Garavito, R.M., Baumeister, W., Rosenbusch, J.P. 1985. Secondary structure of a channel-forming protein. Porin from *E. coli* outer membranes. *EMBO J.* **4:**1589–1592
29. Menestrina, G. 1986. Ionic channels formed by *Staphylococcus aureus* alpha-toxin: Voltage-dependent inhibition by divalent and trivalent cations. *J. Membrane Biol.* **90:**177–190
30. Menestrina, G., Mackman, N., Holland, I.B., Bhakdi, S. 1987. *Escherichia coli* haemolysin forms voltage-dependent ion channels in lipid membranes. *Biochim. Biophys. Acta* **905:**109–117
31. Paul, C., Rosenbusch, J.P. 1985. Folding patterns of porin and bacteriorhodopsin. *EMBO J.* **4:**1593–1597
32. Rosenbusch, J.P. 1988. Secondary and tertiary structure of membrane proteins. *In:* Bacterial Protein Toxins, Zentralblatt für Bakteriologie Suppl. 17. F.J. Fehrenbach, J.E. Alouf and P. Falmagne, editors. pp. 259–266. Gustav Fischer Verlag, Stuttgart—New York
33. Schein, S.J., Colombini, M., Finkelstein, A. 1976. Reconstitution in planar lipid bilayers of a voltage-dependent anion-selective channel obtained from *Paramecium* mitochondria. *J. Membrane Biol.* **30:**99–120
34. Schein, S.J., Kagan, B., Finkelstein, A. 1978. Colicin K acts by forming voltage-dependent channels in phospholipid planar bilayer membranes. *Nature (London)* **276:**159–163
35. Schindler, H., Feher, G. 1976. Branched bimolecular lipid membranes. *Biophys. J.* **16:**1109–1113
36. Schindler, H., Rosenbusch, J.P. 1981. Matrix protein from *Escherichia coli* outer membranes forms voltage-controlled channels in lipid bilayers. *Proc. Natl. Acad. Sci. USA* **75:**3751–3755
37. Tobkes, N., Wallace, B.A., Bayley, H. 1985. Secondary structure and assembly mechanism of an oligometric channel protein. *Biochemistry* **24:**1915–1920
38. Unwin, P.N.T., Ennis, P.D. 1984. Two configurations of a channel-forming membrane protein. *Nature (London)* **307:**609–613
39. Wong, K., Green, M., Buckley, J.T. 1989. Extracellular secretion of cloned aerolysin and phospholipase by *Aeromonas salmonicida*. *J. Bacteriol.* **171:**2523–2527

Received 20 June 1989; revised 5 October 1989